AD-A118 063 AIR FORCE INST OF TECH WRIGHT-PATTERSON AFB OH SCHOO--ETC F/G 7/4
SPECTROGRAPHIC ANALYSIS OF IODINE EMISSION.(U)
JUN 82 J J BAER
UNCLASSIFIED AFIT/GAE/AA/81D-3 NL


A
806

SPECTROGRAPHIC ANALYSIS OF
IODINE EMISSION

THESIS

James J. Baer
AFIT/GAE/AA/81D-3 1Lt USAF

Approved for public release; distribution unlimited.

AFIT/GAE/AA/81D-3

SPECTROGRAPHIC ANALYSIS OF IODINE EMISSION

THESIS

Presented to the Faculty of the School of Engineering
of the Air Force Institute of Technology
Air University
In Partial Fulfillment of the
Requirements for the Degree of
Master of Science

by

James J. Baer
1Lt USAF

Graduate Aeronautical Engineering

June 1982

Approved for public release; distribution unlimited

Preface

The purpose of this thesis was to explore the infrared emissions of iodine behind a strong shock wave in a shock tube. These emissions are the result of dissociating crystalline iodine in the presence of a high temperature and high pressure environment produced by a reflected shock wave. This investigation into the IR spectrum of iodine is a follow-on project first carried out by Captain Lawrence C. Farnell, GAE-80D. His investigation involved determining the IR emission with the use of a wide bandpass filter (1.1μ - ∞) and a liquid nitrogen cooled IR detector. Therefore, it was not possible to determine the exact wavelengths that were observed. This project involves the use of a spectrometer which enables the determination of the excitation frequency down to approximately 50$\mathring{A}$ bandpass. This work has come about due to the Air Force's interest in the possible developing of an efficient mechanism to produce iodine excitation for use in high energy iodine laser application.

My many thanks go out to my advisor, Dr. W.C. Elrod, for his advice during the course of my research, to my thesis committee members, Dr. E.A. Dorko and Dr. H.E. Wright, and to Dr. J.H. Newton at Foreign Technology Division, WPAFB, who sponsored this research. I would also like to thank the Aeronautics and Astronautics department technicians, Mr. W.W.

Baker and Mr. H.L. Cannon for their assistance in time of need. I am also grateful for the advice and equipment given to me for my research by the technical laboratory staff in the Physics Laboratory at AFIT, Mr. J.T. Miskimen, Mr. J.R. Gabriel, and Mr. G.J. Gergal. I am also indebted to Mr. Skip Shepherd at the Aerospace Guidance and Meteorology Center at Newark AFS, for providing needed equipment, and to Mr. Bruce Clay for help in obtaining and building electronic components. A final thank you goes out to Mr. C.M. Phillippi of the Materials Laboratory, Air Force Wright Aeronautical Laboratory, for his advice on experimental procedure, and for the equipment he loaned me to carry out this research.

James J. Baer

Contents

List of Figures

List of Tables

List of Symbols

A	Calibration constant for quartz pressure transducers
$\mathring{A}$	Angstrom
Ar	Argon
ΔA	Distance on oscilloscope traces (cm)
B	Calibration constant for quartz pressure transducers
C	Calibration constant for quartz pressure transducers
D	Distance between downstream pressure transducer and tube endwall (0.5 ft)
ΔD	Distance between shock tube pressure transducers (1.2m)
Δh	Vertical displacement on oscilloscope (cm)
I	Atomic iodine
I_2	Molecular iodine
k	Gas specific heat ratio
K_D	Forward rate reaction constant
K_R	Reverse rate reaction constant
$K_{R_{I_2}}$	Reverse rate reaction formation constant of molecular iodine
M	Mach number
M_x	Third body in a chemical reaction
m	Molecular weight of a gas
ms	Time (milliseconds)
mv	Voltage (millivolts)
MSPCM	Oscilloscope time sweep (milliseconds per cm)
P	Absolute Pressure (psia)

R	Absolute temperature (R°)
$\bar{R}$	Universal gas constant (1554 ft lbf/lb. mole R)
Δt	Time interval (sec)
T	Absolute temperature (R°)
μ	Wavelength (microns)
V	Shock velocity (ft/sec)
WPCM	Oscilloscope sensitivity (millivolts per cm)
ΔX	Distance on oscilloscope traces (cm)

Subscripts

1	Undisturbed test gas in front of advancing shock front
2	Region between shock front and contact surface
3	Region between contact surface and expansion fan
4	Undisturbed driver gas in front of advancing expansion fan
5	Region of test gas that reflected shock wave has passed through

Abstract

The 2-inch I.D. gas dynamic shock tube at the Air Force Institute of Technology, Wright-Patterson AFB, was used to examine the infrared emission spectrum of iodine in the 1.1-1.5μ range. A reflected shock wave passing through the test gas generated the high temperature that was necessary to dissociate the iodine, and cause infrared emissions. Helium gas was used as the driver gas, and argon gas was used in the driven (test) section of the tube. The infrared emission was passed through a grating spectrometer (1200 lines/mm, 121,000 total lines) and was detected at the outlet slit with a liquid nitrogen cooled indium-antimonide IR detector. Control tests were run without iodine to verify that the spectrometer and IR detector were working properly during which time strong argon lines were observed. Subsequent tests revealed the infrared emissions characteristic of iodine in the 1.1-1.5μ range. There is sufficient evidence to suggest that the 1.3151μ electronic mode was excited; however, there may not have been a high enough energy state to extract energy in the lasing mode. The test section condition that was generated during observation of the 1.3151μ line was T_5 of approximately 5000°R.

SPECTROGRAPHIC ANALYSIS OF IODINE EMISSION

I. Introduction

The U.S. Air Force is currently involved in research and effort to establish a more efficient pumping mechanism for the iodine laser. Since power output is directly related to pumping efficiency, increasing this efficiency factor will also increase available power output. There are many ways to produce the excitation that is needed to cause lasing, including exploding wires, electric discharge, gaseous explosions, and chemical reactions. Since the existence of a shock wave is common to some of the above methods, it is plausible that the same result might also be obtained by using a shock tube. This investigation will employ the use of a shock tube to determine the IR spectrum for iodine and, in particular, to see if radiation is stimulated at a wavelength of 1.3151μ, which is of interest for the iodine laser.

Background

Since the inception of the gas dynamic laser (GDL) in 1967, many methods have been tried that produce excitation in different elements. These methods include bunsen burners, electric discharge, flash photolysis, and propagation of shock waves around bullets in flight. Many of the above mentioned

methods can result in carbon formation, surface ignition, and other non-thermal type chemical processes (Ref 3). By using a shock tube many of the problems can be avoided. Also, the temperature produced in a shock tube is not dependent on fuel-air ratio, as it would be in a bunsen burner or spark-ignited gaseous explosion (Ref 3). The shock produced temperature is also a more uniform type environment as the material is almost instantaneously elevated to the desired temperature, held there for a short time, and rapidly quenched by the sidewalls of the shock tube. Such even heating and rapid cooling make the shock tube an ideal tool for use in chemical analysis. Also, since the time interval at elevated temperatures is so short, very high temperatures can be produced without concern over melting the quartz viewing window of the shock tube.

Previous work with iodine excited by a shock wave has been carried out by Britton, et al. (Ref 2). Their work involved the dissociation reaction:

$$M_x + I_2 \underset{K_R}{\overset{K_D}{\rightleftharpoons}} M_x + I + I \qquad (1)$$

where M represents a third body (i.e., argon), and has been investigated using argon and other inert gases in the 1000°-2880°R range. "The ratio $K_{R_{I_2}}/K_{R_{Ar}}$ of the efficiencies of iodine and argon (Ar) as third bodies is not greater than 30 at 2340°R whereas it is 250-600 at room temperature. The hypothesis is proposed that in general the ratio $K_R(gas)/K_{R_{Ar}}$ for complex gases will decrease with increasing temperature [Ref 2:804]."

Problem Statement

The purpose of this thesis is to study the infrared emissions produced when iodine is dissociated in a shock tube. The investigation will cover the wavelength from 1.1-1.5μ since the wavelength of interest for iodine laser development (1.3151μ) is in this range. Since Britton, et al. have shown that iodine can be dissociated with a shock wave, it is plausible that the shock tube could be used to generate the higher temperatures that are necessary to produce excitation of the 1.3151μ line of iodine. This line is an electronically excited mode and, hence, higher temperatures than Britton, et al. used (1890-2880°R) must be generated.

Research Approach

A grating spectrometer was used to make possible the narrow bandwidth analysis of the energy radiated from the test section under the high temperature condition of the investigation. Since gratings are very inefficient in the IR region, conventional attempts at detecting spectrometer light output with a photodiode, photo transistor, or photo pile failed. (This was also due to the fact that a good spectrometer is capable of narrowing down the bandpass to a few angstroms, and a low level signal was entering the spectrometer from the shock tube viewing window.) It was necessary to use a liquid nitrogen cooled indium antimonide IR detector, coupled with a high gain current amplifier to detect the low level signal at the discrete wavelength of the radiation. A lens focused the IR

signal coming from the shock tube onto the inlet slits of the spectrograph. A filter (1.1-1.5μ bandpass) was used at the inlet slits to narrow the bandpass of incoming radiation.

II. Experiment

This section provides the reader with a rudimentary knowledge of how the experiment was carried out and insight into conditions within the shock tube after diaphragm rupture. A detailed list of instrumentation is also included.

Apparatus

The shock tube is configured with quartz pressure transducers located in the test section (Fig 2). One transducer is located directly above the quartz viewing window (downstream transducer), and the second transducer (upstream transducer) is located 1.2 meters upstream. These two transducers provide the information necessary to deduce the shock speed, and also provide a trace of dynamic test section pressure. Iodine crystals are placed on an aerodynamically shaped wedge and mixed with the high velocity test gas behind the passing incident shock wave. The iodine is raised to a very high temperature by the high temperature gas behind the reflected shock. The iodine-gas mixture is brought to rest by the reflected shock wave since the gas velocity behind this wave is zero. The resulting IR signal is extracted through a quartz window in the shock tube, passes through the spectrometer and into an infrared detector. The output voltage signal is then boosted in strength by a high gain current amplifier and is displayed on an oscilloscope along with the pressure trace from the downstream test

section pressure transducer. A second oscilloscope is used to display output from the upstream and downstream test section pressure transducers from which shock speed is deduced. Two photographs are thus obtained, one yielding pressure and IR data, the second yielding both pressure transducer outputs from which time intervals and, hence, shock speeds are determined.

Shock Tube Operation

A shock tube is simply a device in which a shock wave can be artificially produced. The tube used in this project is a 30 ft long by 2 in. I.D. constant area stainless steel tube with 15 ft long driver and driven sections. A mylar or stainless steel diaphragm separates the higher pressure "driver" gas from the lower pressure "test" gas. Relative conditions produced in the shock tube can best be explained by the diagrams in Fig 1.

Immediately after the diaphragm ruptures, the shock front or shock wave is formed and advances out into the test gas which is at rest. A contact surface forms behind the shock wave and it is this surface that forms the boundary between test gas and driver gas (Fig 1b). Station 1 is the undisturbed test gas between the driven end of the tube and the shock front; station 2 is the test gas that occupies the region between the shock front and the contact surface; station 3 is the driver gas between the contact surface and the expansion fan; station 4 is the undisturbed gas between the driver end of the tube and the expansion fan; and station 5 is that region of test gas between

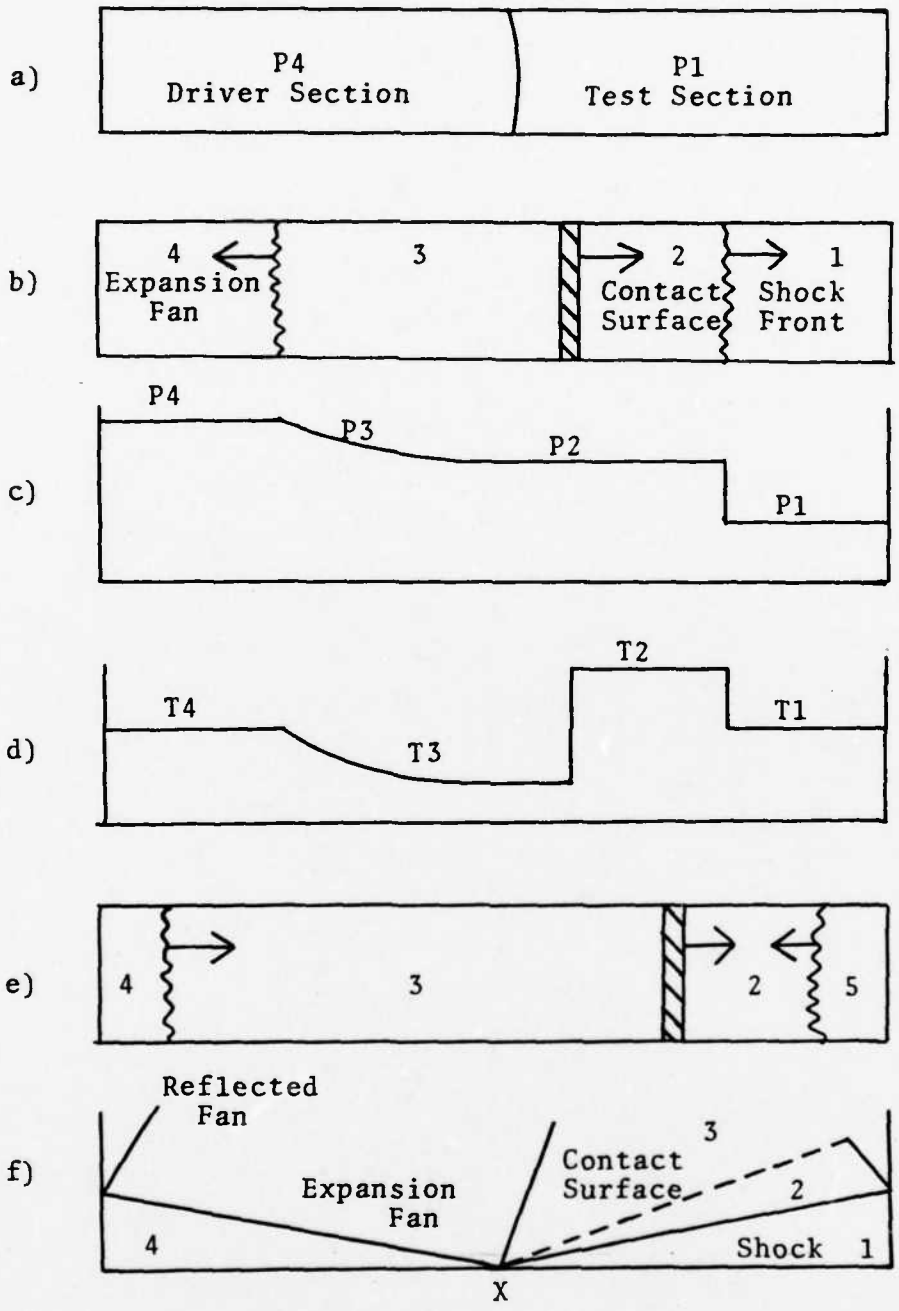

Fig 1. Shock Tube Operating Conditions
(a. Conventional Shock Tube Prior to Diaphragm Rupture; b. After Rupture; c. Pressure Distribution; d. After Shock is Reflected Off Tube End; f. Time vs X Diagram)

the driven end of the tube and the shock front after the shock front has been reflected off the tube endwall. It is this reflected shock that is responsible for creating the high temperatures, since the test gas in region 5 has been heated twice, once by the initial passing shock front, and a second time by the reflected shock front (Fig 1-E). The quartz viewing window is located approximately 8 inches from the test section end of the shock tube.

In shock fixed coordinates the following equations yield the pressure and temperature in region 5 relative to the initial pressures and temperatures in region 1 as a function of shock Mach number and gas properties. Pressure P_1 is directly measured prior to diaphragm rupture, while temperature T_1 is estimated by inserting a thermometer into the test section after a run has been completed.

$$\frac{P_5}{P_1} = \left[\frac{2kM^2-(k-1)}{k+1}\right]\left[\frac{(3k-1)M^2-2(k-1)}{(k-1)M^2+2}\right] \qquad (2)$$

$$\frac{T_5}{T_1} = \frac{[2(k-1)M^2+(3-k)][(3k-1)M^2-2(k-1)]}{(k+1)^2M^2} \qquad (3)$$

The Mach number (M_1) in these two equations may be determined in one of two different ways: 1) by direct calculation employing sensor data of time interval required for shock to pass two reference points; or 2) by use of the following ideal gas equation that related driver and driven section pressures prior to diaphragm rupture;

$$\frac{P_4}{P_1} = \left[\frac{2kM^2-(k-1)}{k_1+1}\right]\left[1 - \frac{k_4-1}{k_1+1}\left(\frac{a_1}{a_4}\right)\left(M - \frac{1}{M}\right)\right]^{-\left(\frac{2k_4}{k_4-1}\right)} \qquad (4)$$

The Mach number may be solved for by trial and error or by employing a numerical method such as the secant method. The normal procedure is to take the actual Mach number as determined by sensor data, and to determine P_5 and T_5 using Eqs (2) and (3). This will avoid compounding of errors, since the actual Mach number will be different from the theoretically predicted Mach number (due to real gas effects) as obtained by using Eq (4). A much more thorough approach to shock tube theory may be found in Ref. 3.

Instrumentation

Table I is a synopsis of the major pieces of test equipment and associated support equipment that were used. The basic pieces of equipment will be explained in later sections. This explanation will be supplemented with photographs and schematics where appropriate.

Particle Injector

The device used to "load" the crystalline iodine into the test section is called a particle injector. A photograph of this injector can be seen in Fig 3. The aerodynamically shaped wedge can be seen at the mouth of the tube. The iodine crystals are placed on this wedge, and the assembly placed into the test section of the shock tube. The passing shock wave and

TABLE I

Instrumentation and Support Equipment

The following is a list of all major pieces of instrumentation used in this thesis. This equipment is shown schematically in Fig 2.

Item	Description	Model #	Serial #	Use
1	CMC Electronic Counter	726C	--	Time shock wave
2	Tektronix Oscilloscope	551	--	Display IR trace and test section pressure
3	Camera	--	--	Photograph IR trace and test section pressure
4	High Gain differential amplifier	1A7A	13051412	Amplify IR detector output voltage
5	High Gain differential amplifier	1A7A	13063028	Amplify test section pressure pulse
6	Tektronix Oscilloscope	551	--	Display test section pressures
7	Camera	--	--	Photograph test section pressure trace
8	High Gain differential amplifier	1A7A	13062442	Amplify downstream pressure transducer output
9	High Gain differential amplifier	1A7A	13063027	Amplify upstream pressure transducer output
10	Vacuum pump	--	--	Evacuate shock tube
11	Vacuum pump	--	--	Evacuate shock tube
12	Shock tube	--	--	Produce shock wave
13	Focusing lens	--	--	Focus IR signal output into spectrograph
14	Bandpass filter	--	--	1.1-1.5 bandpass filter
15	SPEX Spectrograph	1702	2586	Break incoming signal into component colors
16	Barnes Engineering IR detector	--	0797	Detect IR radiation
17	Kiethely Current amplifier	427	83119	Amplify IR detector output
18	Shock tube remote control board	--	--	Provide remote tube operation
19	Systron Donner Digital multimeter	7000A	1712	Digital output for Viatran pressure transducers

TABLE I, continued

Item	Description	Model #	Serial #	Use
20	Hewlett-Packard dual power supply	6205B	1020	Provide power to Viatran pressure transducers
21	Systron Donner digital multimeter	7000A	1633	Digital output for Viatran pressure transducers
22	Lambda power supply	LK343FM	--	Provide power to control board
23	Kistler charge amplifier	566	1752	Amplify quartz pressure transducer signal
24	Kistler charge amplifier	566	3466	Amplify quartz pressure transducer output
25	Viatran pressure transducer	104	150160	Measure pressure in driver section (P_4)
26	Viatran pressure transducer	104	150150	Measure pressure in driven section (P_1)
27	Kistler quartz pressure transducer	603A	1701	Measure downstream driver pressure
28	Kistler quartz pressure transducer	603H	1158	Measure upstream driver pressure

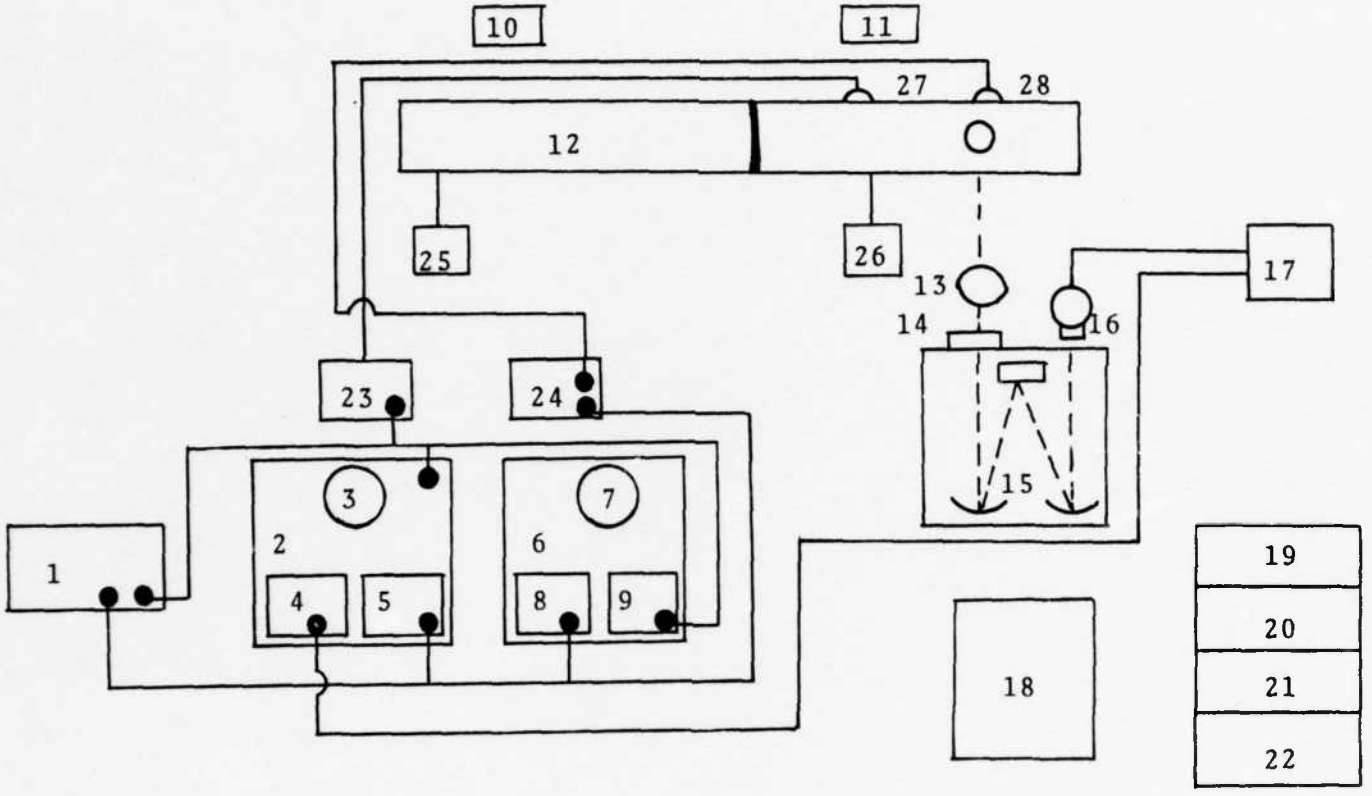

*Numbers Referenced to Table I

Fig 2. Major Support Equipment

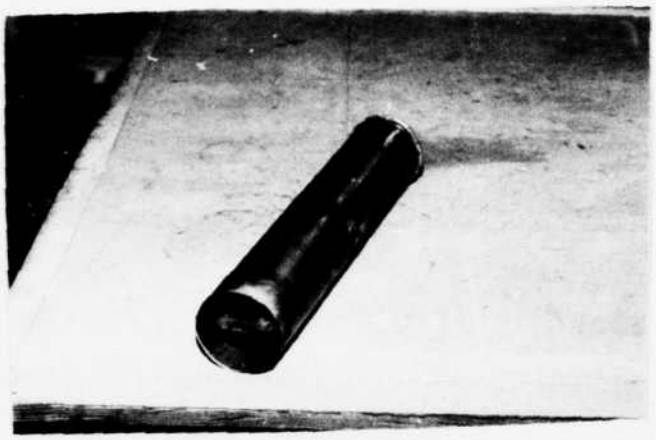

Fig 3. Photograph of Particle Injector

gas flow then sweep the iodine off the wedge and disperse it downstream. The hole on the side of the tube (also a hole on the far side) lines up with the shock tube window to provide an optical path from the radiation source to the signal detector. The smaller hole at the top of the particle injector tube is so that the downstream pressure transducer may be made flush with the inside surface of the test section to optimize its response to the shock front.

Grating Spectrometer

The basic principles of grating spectrometers have long been in the literature. A thorough coverage of this subject may be found in Ref. 2. The spectrometer used in this research has 1200 lines/mm with 121,000 total lines, and can resolve the two spectral lines of the sodium doublet at 5330Å (i.e., 5330.1Å and 5330.5Å). The resolution at 1.0μ is estimated to be less than 25Å. It is also known that "very large theoretical resolving powers are, in fact, very nearly attained in

practice throughout the visible and ultraviolet portions of the spectrum, but in the infrared these theoretical resolving powers are seldom realized [Ref 4: 462]."

IR Detector

The IR detector used in this research is a solid state device employing a diffused p-n junction (Ref 1). It is operated at cryogenic temperatures (liquid nitrogen 139°R). An advantage of using this type of detector is that it has a much greater sensitivity than those detection devices that are not cryogenically cooled, but yet the detector can be used as a conventionally uncooled device. The detector is operated as an active device and, as such, no bias current need be supplied to the detector. The general shape of the response curve, that is typical of such devices, resembles that of a parabola. Within the wavelength of investigation of this research (1.1-1.5μ), the curve can be assumed to be linear with only a slight deviation from its true shape (assuming a linear response curve permits a comparison of output voltages for signals originating from different wavelengths).

There are three main problems associated with using this type of detector. First, the detector is temporarily "blinded" if it is exposed to radiation of less than 1μ prior to being cooled with liquid nitrogen. This blinding results in an almost 100 percent drop-off in voltage output for weak input light signals. This blinding is only temporary, and can be alleviated by warming the detector assembly to room

temperature, shielding the detector from radiation of less than 1μ, and then cooling down with liquid nitrogen (Ref 1). Second, there is the problem of spurious electronic noise in the detector signal input to the oscilloscopes. Much of this is from the detector, and some noise can also be attributed to the current amplifier that was used to amplify the IR detector output signal. Some of this noise was eliminated by "floating" (disconnecting) the ground connections of the current amplifier and of the oscilloscope that displayed the IR trace. It was also found helpful to shield the detector with aluminum foil to block out stray electromagnetic radiation. Third, there is a minor problem of output drift from the detector signal. Trace drift is evident even after several hours of system stabilization (i.e., after detector has been cooled down with liquid nitrogen, shielded with aluminum foil, and allowed to remain undisturbed for several hours). Trace drift is actually an A.C. signal with very low frequency. Since the frequency of the IR trace is much greater than that of the drift signal coming from the detector, this noise can be eliminated by switching the oscilloscope low cut-off frequency from D.C. to 0.1 c.p.s. A.C. Spurious A.C. signals are now effectively blocked, yet normal IR output signals can still be displayed.

Optics

In Fig 4 a diagram of the optical system that was used in this project is shown. The shock tube viewing window is made of ground quartz glass with a transparency range from

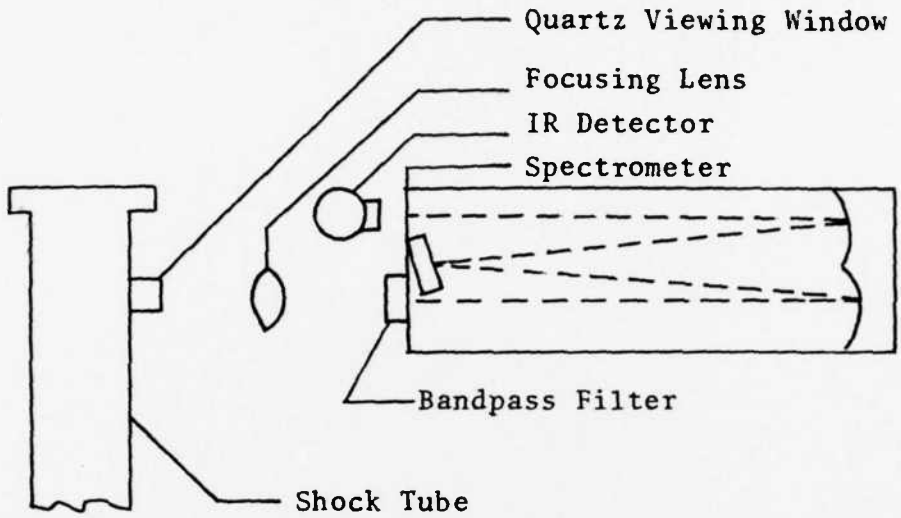

Fig 4. Optical Configuration

the visible up to 2.7μ. The signal then passes through a glass focusing lens and then through a 1.1-1.5μ bandpass filter. This filter is shielded from stray electromagnetic radiation by surrounding the inlet of the spectrometer with aluminum foil. The IR signal then passes through the inlet slit of the spectrometer and is reflected off the first of two internal parabolic mirrors. The signal is then refracted into its spectrum at the grating face, reflected off the second parabolic mirror, and finally the selected wavelength exits at the outlet slit where the IR detector received the signal. The detector is suspended from a three degree of freedom mount and covered with multiple layers of aluminum foil to shield

the detector eye from stray electromagnetic radiation.

Tank Farm and Cold Traps

Figure 5 shows the tank farm system that was used to pressurize the driver end of the shock tube. Desired tube pressure is achieved in three increments. Tank #1 boosts pressure up to 40 percent of final value, tank #2 boosts to 75 percent, and tank #3 boosts to diaphragm rupture pressure. By elevating pressure in three steps, more runs can be completed before bottles need to be replaced. When bottle #3 drops below maximum desired bottle pressure, the bottles are rotated with #3 becoming #2, #2 becoming #1, and #1 being replaced with a fresh bottle (i.e., becoming #3). Continued rotation ensures that maximum use is obtained from all cylinders before being changed. Maximum shock tube pressure capability is approximately 10,000 psia, however actual operating limit is 2,200 psia, which corresponds to maximum bottle gas pressure available. A booster pump would be necessary to go beyond this limit. The test section of the tube was pressurized to very low levels (approximately atmospheric) and, therefore, a tank farm system for the test gas was not required. A single argon tank was sufficient for all runs. Not shown are vacuum pumps used to evacuate both ends of the shock tube. Vacuum readings were obtained with a mercury manometer.

Cold traps were used to separate iodine from the gas mixture prior to releasing the mixture to the atmosphere. Iodine is collected by condensation on the cold sidewalls of

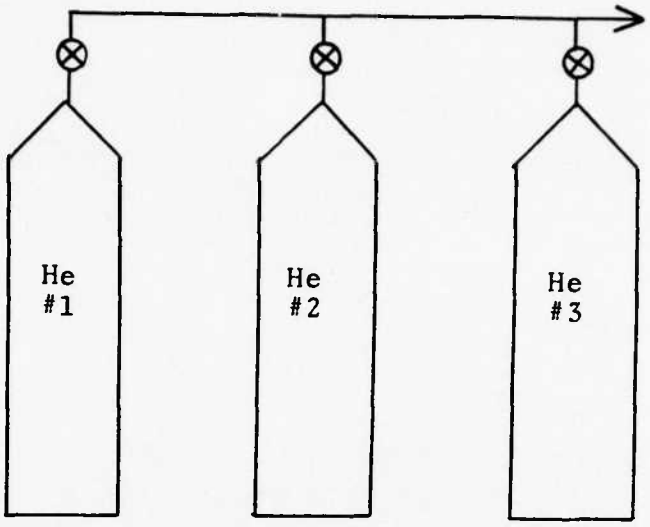

Fig 5. Helium Tank Farm System

the traps. Traps were cooled with a mixture of dry ice and alcohol.

III. Procedure

Proper procedure must be followed to ensure that results are consistent and reliable. Of paramount importance is instrument calibration and alignment of optical systems. In this investigation, in addition to calibration of instrumentation, trial runs were made to insure repeatability of the experiment and the data.

Instrument Calibration

Viatran Pressure Transducers. Viatran pressure transducers were used to measure pressures in the driver and driven sections of the shock tube prior to diaphragm rupture. These transducers provide a voltage output that is proportional to applied pressure. Consequently, a calibration curve was obtained for each of two transducers. A linear calibration curve as in Eq (6) resulted for each transducer.

$$\text{Gauge Pressure} = A \cdot (\text{transducer output voltage}) + B \quad (6)$$

The constants A and B represent the slope and intercept and are slightly different for each of the two transducers. These transducers were calibrated up to 2000 psig with an oil-filled dead-weight tester.

Kistler Quartz Pressure Transducers. Measurement of rapidly varying test section pressures was accomplished with the use of a pair of quartz pressure transducers. These

transducers employ the concept of piezoelectric response, providing a capacitive signal proportional to applied pressure. One transducer was located directly above the quartz observation window, the other 1.2m upstream. A calibration curve can also be obtained for the quartz transducer and charge amplifier combination.

$$\text{Gauge Pressure} = C \cdot (\text{charge amplifier output voltage}) \quad (7)$$

where C is a calibration-derived constant. These transducers were calibrated up to 2500 psig with an oil-filled dead-weight tester.

Spectrometer. Spectrometer calibration was accomplished in three steps: 1) wavelength calibration; 2) bandpass calibration; and 3) linearity calibration. Wavelength calibration involved setting the machine dial of the spectrometer at a wavelength for which a spectral line source was available (neon pen lamp). Rotation of the machine dial then led to a visual determination of the brightest area and, therefore, the peak wavelength of the light source. The difference between the known wavelength and the indicated wavelength by the spectrometer dial is the amount by which the spectrometer is out of calibration. While this seems like a crude calibration method, it must be remembered that the human eye is quite sensitive in the visible range, much more so than are most photo transistor devices. The machine was calibrated in the near infrared region of the spectrum by using the same light source as was used above. This resulted in

performing a second order calibration (i.e., a 6000Å red line is also seen as a red line when the spectrometer dial is set at 12,000Å. A third order calibration could also have been performed in which case the 6000Å red line would be observed at a setting of 18,000Å, etc.).

Next a bandpass calibration was performed. This involved the use of a lightbulb, a bandpass filter, and the infrared detector. The spectrometer dial was set to the peak wavelength of the bandpass filter, and the slit width opened to maximum value. The wavelength dial is then rotated in one direction until the IR detector output goes to zero, at which point the dial reading is recorded. The same process is repeated, but in the opposite direction. The wavelength difference between these zero output values is an indication of the bandpass at a given slit width. The same process is again repeated at a different slit width. Now a graph of $\Delta\lambda$ vs slit width can be drawn. A linear relationship was obtained.

Finally, a relative intensity calibration was performed. This calibration determines the linearity of the detector response to light at fixed wavelengths but varying intensities. This process was performed by exposing the detector to light of one wavelength, and sliding a clear glass plate between the detector and the light source. Glass will block approximately 10 percent of this light and, therefore, a new detector output voltage can be obtained for light that is now approximately 90 percent its original intensity. A second cover glass is now placed between the detector and the light source,

and a second detector output voltage can be obtained, but now it is for light that is approximately 81 percent its original intensity. The process is repeated and the results of relative light intensity vs detector output voltage are graphed. The resulting curve is a straight line, thus indicating that the detector response to light of fixed wavelength but different intensities is linear. (The percentage of light that is transmitted by a single cover glass is approximately 90 percent, however this value need not be known at all. It only matters that each added cover glass transmit the same percentage of light as the first cover glass did.)

IR detector alignment was performed on a trial and error basis. The detector has to be cooled down and shielded with foil and, therefore, it is not possible to see the face of the detector to perform an alignment. The following procedure was, therefore, used to align the detector for maximum signal output. A 150-watt lightbulb was placed up against the back window of the shock tube test section (bulb was marked with a white circle on the glass surface to ensure that the bulb could be repeatably placed back against the shock tube window in exactly the same position.) The detector is mounted on a 3-way traversing device to allow for proper alignment, cooled down, shielded, and arranged for voltage output to be displayed on an oscilloscope. The spectrometer wavelength dial is then set to an arbitrary setting and the lightbulb turned on. IR detector is then moved around to various positions in order to maximize signal output to the oscilloscope. This procedure can be

repeated with great accuracy. In repeating the alignment procedure, proper alignment is again achieved when the same voltage deflection is seen on the oscilloscope. This calibration light source should not be left on for long periods of time because the detector heats up and the zero reference line drifts.

Optical Alignment

Optical alignment consisted of alignment of focusing lens, spectrometer, and IR detector with shock tube viewing window. Coarse adjustment was achieved by using a 15 mw helium-neon laser (Fig 6). The back window of the shock tube was removed and the laser beam centered through the two shock tube holes. The beam was then centered through the focusing lens onto the spectrometer inlet slits. The top covers of the spectrometer were removed to facilitate centering of the incoming beam onto the two parabolic mirrors and for even dispersion on the grating face. The beam was then checked for proper alignment with the exit slits.

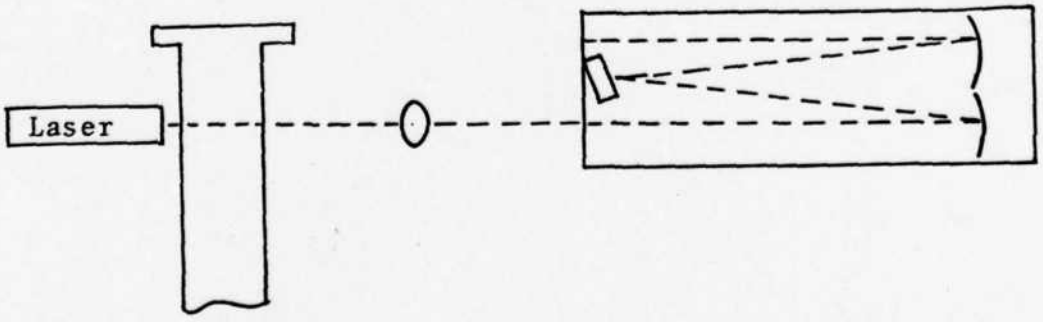

Fig 6. Laser Alignment

Measurement Procedures

Measurement procedures consisted of the following routine. Switch on all equipment and cool down and align the detector. Place diaphragm in holder, insert in shock tube and close up tube. Evacuate driver and driven sections to 1 in. mercury using vacuum pumps, then refill test section to desired pressure with argon test gas. Push ground buttons on charge amplifiers and zero all traces on oscilloscopes. Set scopes in external triggered single sweep mode and set shutter open on cameras. Fill driver section with helium from tank farm system until diaphragm ruptures. Record P_1 and P_4 at rupture, vent tube using cold traps, release camera shutters, develop pictures, and proceed with next run.

IV. Data Reduction

Data reduction consists of determination of shock velocity, Mach number, test section pressure, and temperature estimation. Theoretical values are determined for the same initial conditions for a comparison with the experimental results.

Shock Velocity and Mach Number

Actual shock velocity is measured by timing the shock as it traverses the distance between the downstream transducer to the endwall of the tube and back to the downstream transducer (i.e., by timing the incident and reflected shock wave). This time interval is proportional to the distance shown as ΔX in Fig 7. The method of timing the shock as it passed the

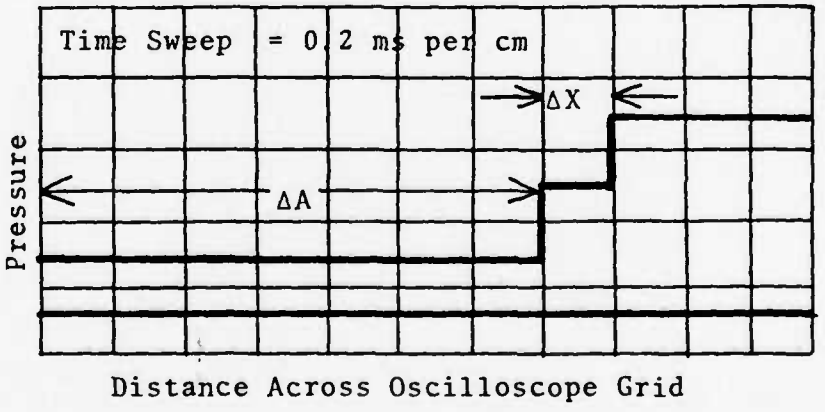

Fig 7. Typical Oscilloscope Time Trace

upstream and downstream transducer (represented by ΔA in Fig 7) was not employed because of a delay in oscilloscope triggering that was frequently encountered. By referencing shock speed to the distance ΔX, any delays in triggering are effectively negated. Using the incident-reflected method to measure shock speed resulted in better data reduction, although this procedure required the aid of the computer. The determination of each velocity required the use of many equations and employed a trial and error procedure, as described below. An incident Mach number is assumed for the wave traveling down the end of the tube. From this assumed Mach number the time for the wave to progress from the downstream transducer to the tube endwall is calculated (t_1). Using this assumed Mach number allows the reflected Mach number to be calculated. The velocity of this reflected wave (relative to the fixed coordinates of the shock tube) can then be determined as the reflected velocity minus the velocity of the oncoming stream of gas. This relative velocity is then used to calculate the time for the reflected wave to traverse the distance from the tube endwall back to the downstream transducer (t_2). If the assumed Mach number was indeed correct, then the sum of t_1 and t_2 should be equal to the time interval represented by ΔX on Fig 7. If the time intervals are different, an iteration must be performed until convergence is obtained and the correct Mach number has been deduced. The equations and procedures used to determine the Mach number are as follows.

Step #1: Assume an incident Mach number for the shock wave traveling down the tube.

Step #2: Using

$$M_1 = \frac{D/t_1}{\left(\frac{k\bar{R}T_1 g_c}{m}\right)^{1/2}}$$

determine t_1 (time for shock to traverse distance between downstream transducer and tube endwall). D is the distance between the downstream transducer and the tube endwall.

Step #3: Determine T_2 (the temperature environment that the reflected shock wave must pass through) by the following equation

$$T_2 = \frac{(kM_1^2 - \frac{k-1}{2})(\frac{k-1}{2}M_1^2 + 1)}{(\frac{k+1}{2})^2 M_1^2} \cdot T_1$$

Step #4: Determine the velocity of the reflected shock wave relative to the oncoming stream of gas

$$V2 = 2\left(\frac{k\bar{R}T_1 g_c}{m}\right)^{1/2}(M_1 - \frac{1}{M_1})$$

Step #5: Calculate the Mach number of the reflected shock wave

$$\sqrt{T_1}(M_1 - \frac{1}{M_1}) = \sqrt{T_2}(M_R - \frac{1}{M_R})$$

where M_R = reflected Mach number

M_1 = assumed incident Mach number

Step #6: Calculate the speed of the reflected wave from

$$V_R = M_R\left(\frac{k\bar{R}T_2 g_c}{m}\right)^{1/2}$$

Step #7: Calculate the speed (V_{ACT}) of the reflected Mach wave relative to the shock tube from

$$V_{ACT} = V_R - V_2$$

Step #8: Calculate the time (t_2) for the reflected wave to travel from the tube endwall back up to the downstream transducer using

$$M_R = \frac{D/t_2}{\left(\frac{k\bar{R}T_2 g_c}{m}\right)^{1/2}}$$

Step #9: Check to see if the following relationship holds

$$(\Delta X) \cdot (MSPCM) = t_1 + t_2$$

where the product on the left-hand side is the time interval represented by the distance ΔX shown in Fig 7.

Step #10: Return to Step #1 and assume a new Mach number. Continue this iteration until the equality in Step #9 is satisfied.

Shock Wave Pressure Determination

Test section pressure may also be obtained from oscilloscope photographs, but in a more straightforward method than was employed to determine Mach number. In Fig 8 the IR trace is the bottom trace, and the test section pressure is on the

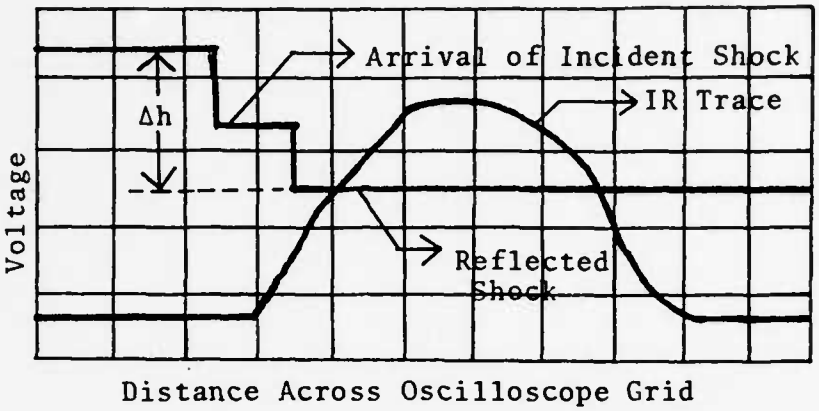

Fig 8. Typical Oscilloscope Trace of IR Signal (bottom) and Test Section Pressure
Timesweep = 0.5 milliseconds per cm
Vertical Sensitivity = 500 millivolts/cm

top trace. (Note that this is not the same photograph from which shock speed was determined. Although shock speed can also be obtained from Fig 8, test section pressures cannot be obtained from Fig 7.) Test section pressure is given by the following relationship.

$$P_5 = P_1 + (\Delta h) \cdot (VPCM) \cdot (.2961) \qquad (8)$$

assuming P_1 = 14.7 psia, VPCM = 500 mv/cm, Δh = 2 cm (Fig 13).

$$P_5 = 14.7 + (2) \cdot (500) \cdot (0.2961 \text{ lbf}/(\text{in}^2 \cdot \text{mv})$$

$$= 311 \text{ psia} \qquad (9)$$

Shock Wave Temperature Determination

Shock tube temperature is extremely hard to measure directly because of the rapidly changing thermal environment. Conventional thermocouples do not possess the high heat transfer rates and frequency response that are necessary for accurate temperature measurement. Therefore, the actual test section

temperatures can only be estimated by use of the following equation.

$$\frac{T_5}{T_1} = \frac{[2(k-1)M^2 + (3-k)][(3k-1)M^2 - 2(k-1)]}{(k+1)^2M^2} \qquad (10)$$

where T_5 is the test section temperature after reflected shock front arrival, and T_1 is the test section temperature prior to diaphragm rupture. This equation does not take into account the presence of iodine, but it is a theoretical upper limit. The addition of a foreign substance, such as iodine, will reduce the temperature rise of the surrounding test gas because the iodine will absorb energy from the gas. This energy is absorbed because energy is required to sublime the iodine, raise its temperature, and possibly to raise it to a dissociated or electronically excited state.

V. Results

The object of this project was to investigate the infrared spectrum of iodine in the 1.1-1.5μ range. To insure the accuracy of these results, the strong spectral lines of the test gas (argon) were first obtained. After the strong argon lines were recorded, other lines that might possibly belong to iodine were more easily recognized. Very strong signals were detected while observing the 1.3151μ iodine line.

Argon Spectral Lines

All seven of the strong argon lines were detected during the base data collection period. There are 48 significant argon spectral lines in the 1.0-1.5μ range. Of these 48 lines, seven are dominant, rating a 400 or more on a 0-1000 relative intensity scale.

Iodine Spectral Lines

A very strong signal was observed at the 1.3151μ iodine line, indicating that the 1.3151μ electronic transition line of iodine was observed. This line was again observed with the same results being obtained. It remains to be determined whether the energy level present is sufficient to permit establishing a laser device.

The photographs in Figs 9 and 10 display the IR trace and shock speed trace that were obtained while observing the 1.3151μ

line of iodine (the experiment was repeated).

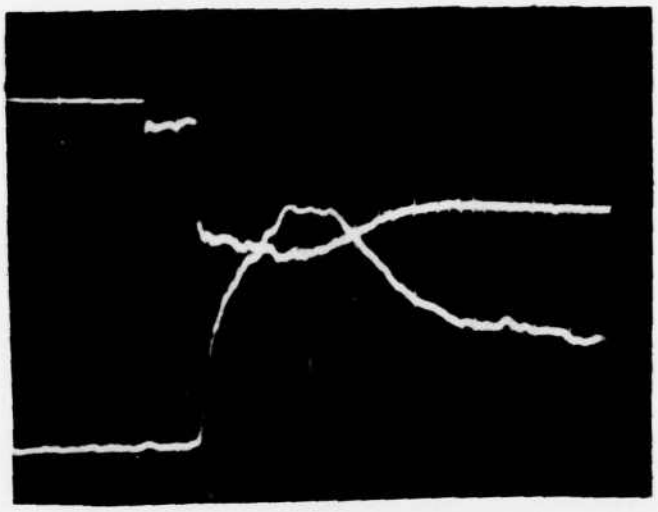

Fig 9. Photograph of IR Trace (bottom) and Test Section Pressure Pulse (top)

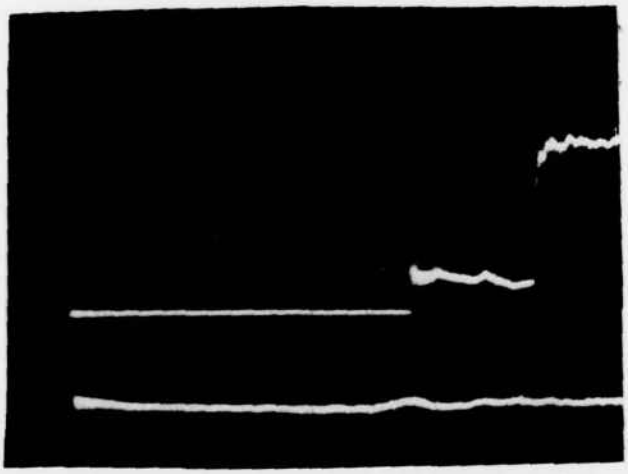

Fig 10. Photograph of Time Trace Used to Compute Shock Velocity

Figures 11 and 12 are plots of pressure ratios versus Mach number. Figure 11 plots P_4/P_1 against Mach number. The solid line represents the ideal line that the data points should fall on. It is normally expected that for P_4/P_1, ratios below approximately 10,000, that the actual Mach numbers will be slightly less than the theoretical Mach numbers (Ref 3). It can be seen from Fig 11 that most of the plotted values adhere to this line of reasoning. Figure 12 displays P_5/P_1 versus Mach number. It can be seen that the actual pressure ratios deviate somewhat from the theoretical predicted values. The plotted values that deviate from the theoretical value by more than one Mach number (at any specific pressure ratio) may be assumed to be poor data points. These "poor data" points represent only approximately 8 percent of the total points.

Figure 13 displays IR detector output voltage as a function of time after reflected shock arrival. This is plotted at 1.3151μ with and without iodine. It is clearly displayed that a significant output is detected when iodine is added. This data was repeated with the same results. The only other line that exceeded the intensity of the 1.3151μ iodine line was the far removed 1.3367μ argon line.

Table II represents the significant spectral lines of iodine and argon. The wavelengths are listed along with their relative intensities on a scale running from 0-5000. Table III displays the iodine and argon lines, and the distance away each is from its nearest neighbor. Notice that the nearest neighboring iodine line to the 1.3151μ iodine line is located

more than 800Å away. It is, therefore, highly unlikely that another iodine line was also being observed at the time the 1.3151μ line was being looked at (remember that the bandpass for the spectrometer is only 50Å at the setting being used). The nearest argon line is located 65Å away, therefore, it is unlikely that an argon line was also being observed. The same has been done for the argon lines. The 1.0467μ iodine line has a very strong argon line only 3Å away. It is, therefore, possible that the resulting output of the detector is due to the argon and not the iodine. However, in the case of the 1.3151μ iodine line, this is not possible.

Table IV displays the significant test runs using argon and iodine. It can be observed that the detector output voltage on the run using iodine greatly exceeds those maximum voltages on the runs using no iodine (at 1.3151μ). The last value (run 21) was inserted to show that, while there was an output voltage that exceeded the value obtained using iodine, this was the result of observing a very strong argon line. However, this wavelength is so far removed from the 1.3151μ iodine line, that it could not possibly be influencing the observed output at 1.3151μ.

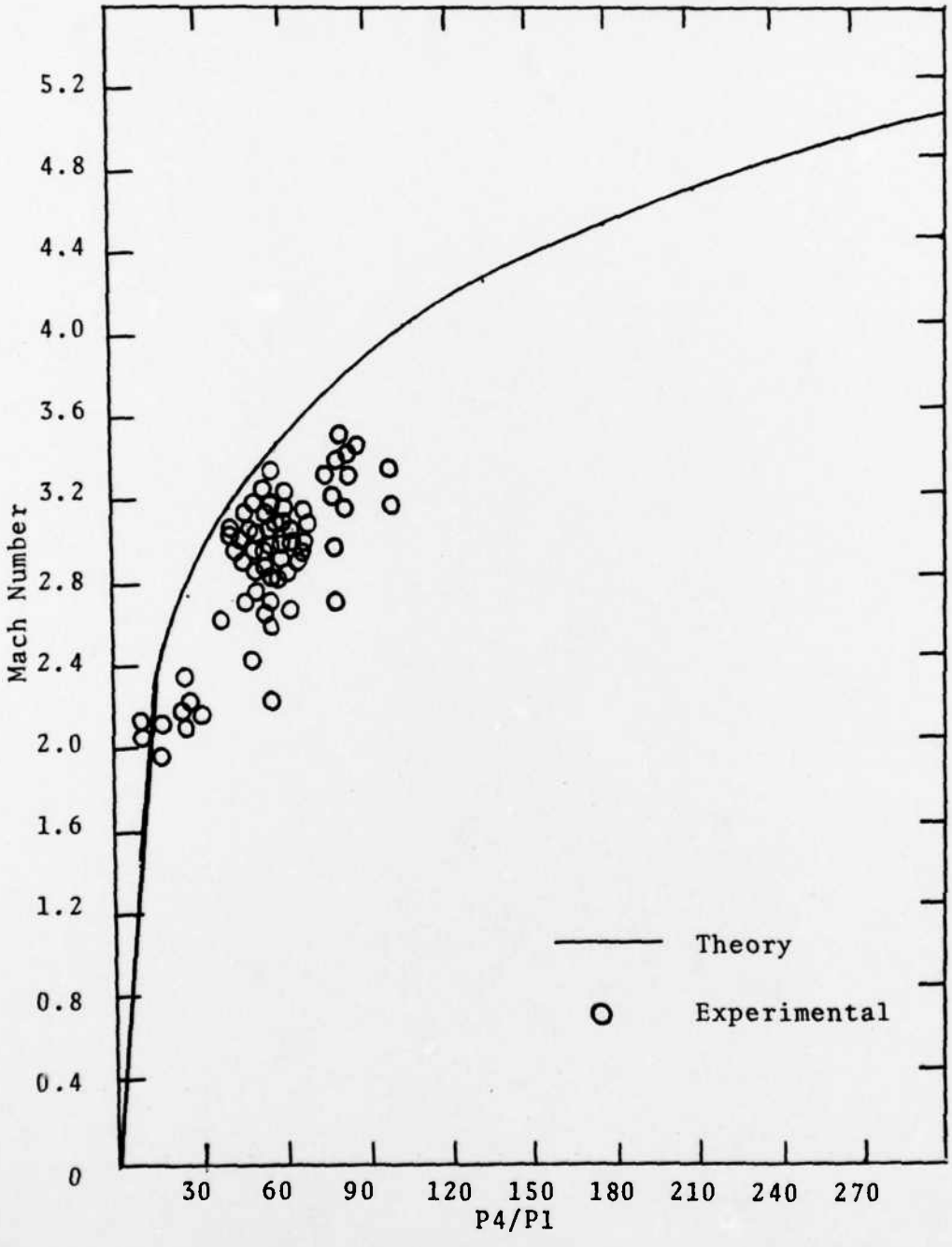

Fig 11. P4/P1 vs Mach Number

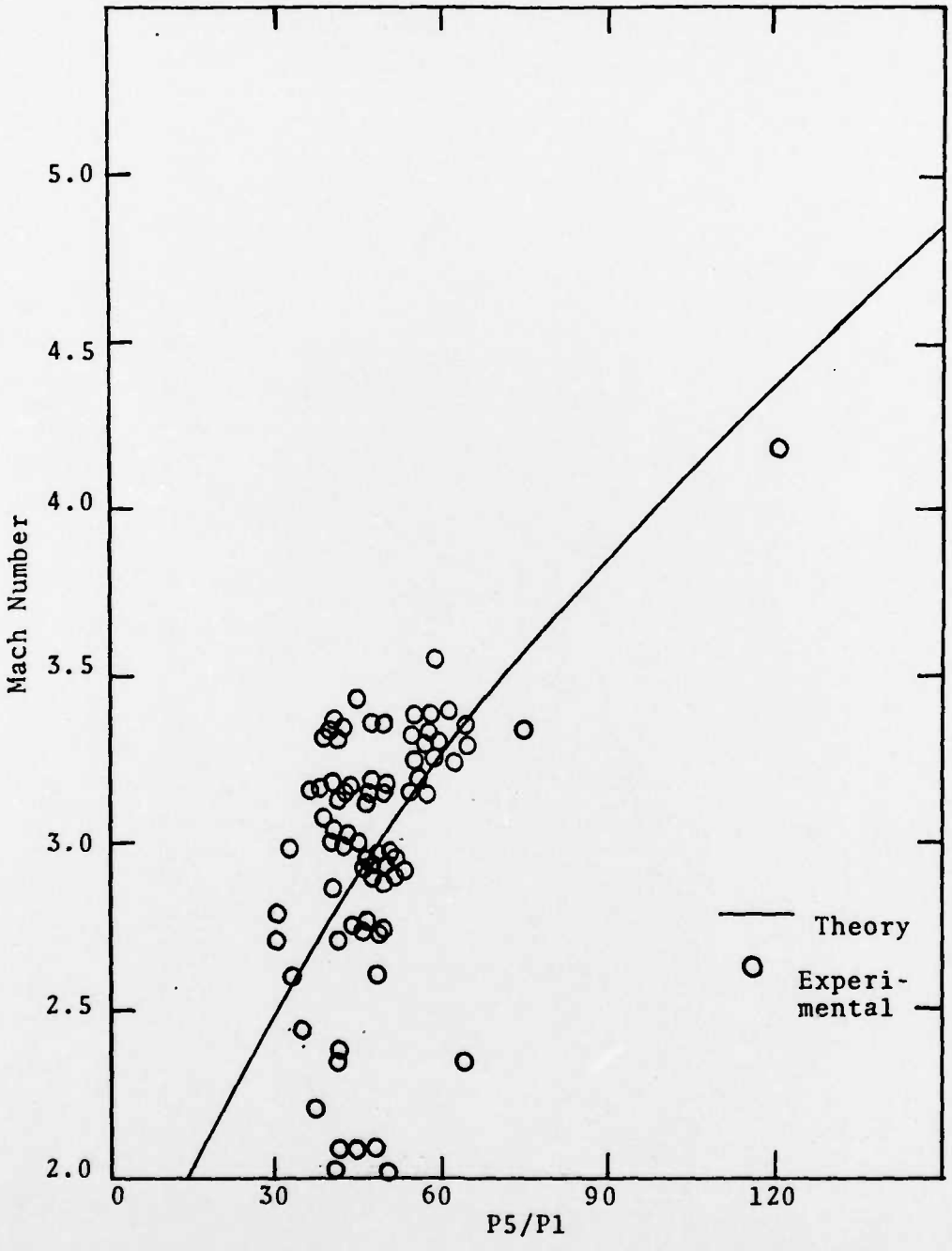

Fig 12. P5/P1 vs Mach Number

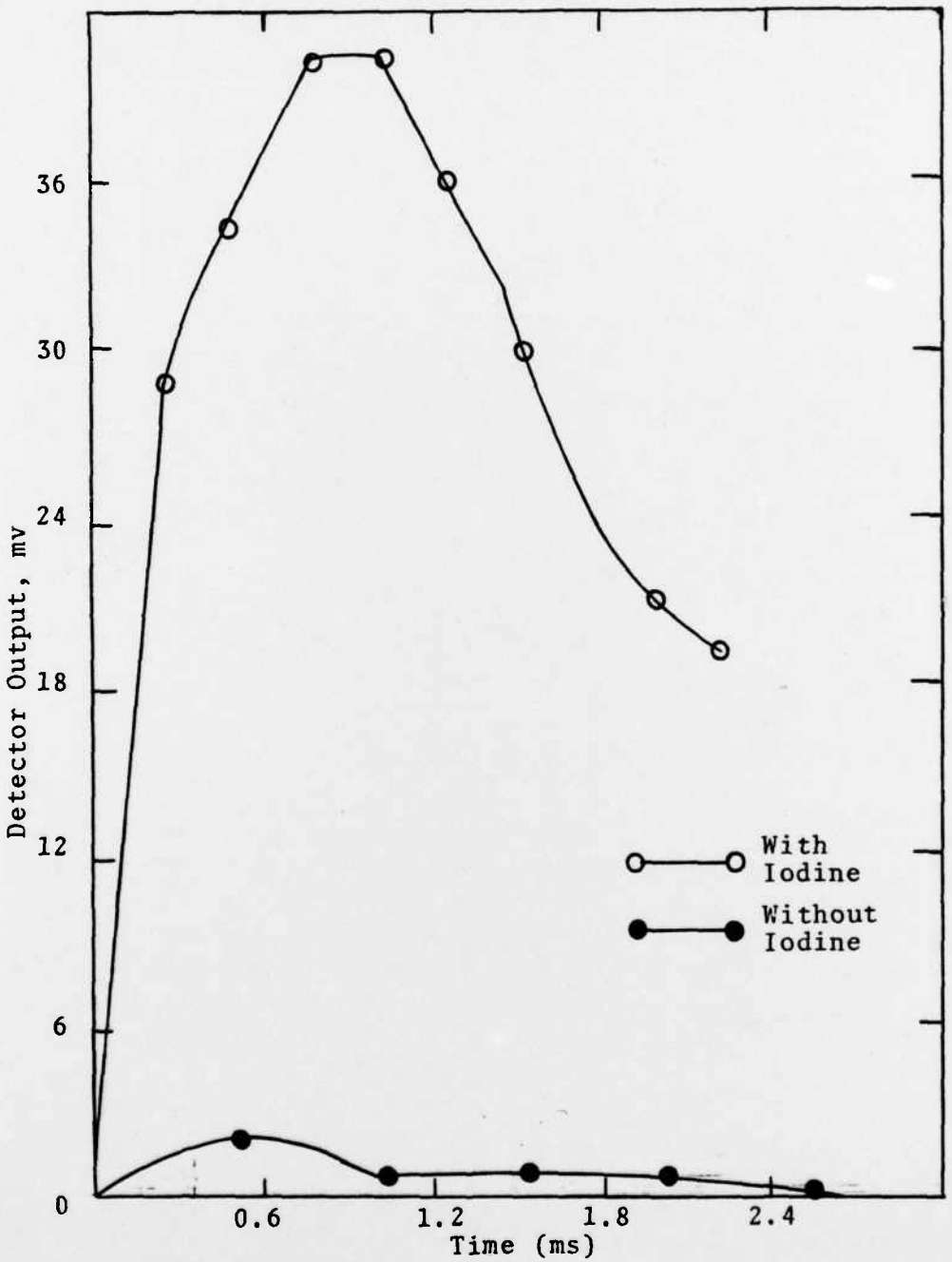

Fig 13. Time After Reflected Shock Arrival vs Detector Output Voltage With and Without Iodine at 1.3151μ

TABLE II

Observed Iodine Lines and Distance Away From Nearest Neighboring Spectral Line

Line Observed Å	Relative Intensity	Distance Away Nearest Neighbor ±(Å)	Relative Intensity	Distance Away Nearest Argon Ln ±(Å)	Relative Intensity
10,239	1000	-108 +136	750 400	-187 + 94	180 130
10,467	5000	- 61 +618	6 1	- 0 + 3	100 1600
13,149	60	-844 +809	150 140	-141 + 65	200 200

TABLE III

Observed Argon Lines and Distance Away From Nearest Neighboring Spectral Line

Line Observed Å	Relative Intensity	Distance Away Nearest Neighbor ±(Å)	Relative Intensity	Distance Away Nearest Iodine Ln ±(Å)	Relative Intensity
10,470	1600	- 3 + 8	100 13	- 3 +615	5000 1
11,488	400	- 46 +181	12 200	-251 + 70	400 350
12,956	500	- 23 + 52	50 200	-922 +49	300 150
13,313	1000	- 40 + 54	500 1000	-164 +645	60 140
13,367	1000	- 40 +132	1000 30	-218 +691	60 140
13,504	1000	- 5 + 70	30 11	-355 +454	60 140
13,719	1000	- 41 +107	200 10	-570 +239	60 140

TABLE IV

Significant Test Data

Run #	λ(μ)	Iodine	Maximum Detector Output Voltage (mv)
106	1.3151	No	2.5
107	1.3151	No	2.1
119	1.3151	Yes	40.0
120	1.3151	Yes	38.0
21	1.3367	No	75.0

VI. Conclusions and Recommendations

Conclusions

The shock tube was used in conjunction with a spectrometer and an infrared detector to observe the emissions of iodine in the 1.0-1.5μ range. The suitability to conduct this investigation is based on the test runs conducted with argon gas alone, and later with iodine and argon. Close attention to instrumentation calibration ensured that this suitability was maintained throughout the experiment. Three lines were observed that would be attributed to the presence of iodine (1.0239μ, 1.0467μ, 1.3149μ). The 1.0239μ and 1.3151μ iodine lines were far enough removed from any other argon or iodine lines that the appearance of a signal was most likely due to these iodine lines alone; specifically, the 1.3151μ electronic mode of iodine was observed, however there may not have been a high enough energy state to extract energy in the lasing mode.

Recommendations

The use of such a large shock tube for this research presented many problems that could be eliminated by using a smaller shock tube system. The large driver end of the tube required using large quantities of helium gas for each run. Employing a much smaller shock tube would permit many more runs per bottle of helium gas. The use of a smaller tube would permit the use of smaller and less costly diaphragms, and reduce the

draw down time with the vacuum pumps. The following recommendations are, therefore, made:

1) Use of a smaller shock tube system. This will significantly reduce direct cost of shock tube operation because less helium and test gas will be used and smaller diaphragms may be used.
2) Use test gas that has no emission lines in the IR region of iodine (argon has emission lines in the vicinity of some of the iodine lines, hence many test runs were necessary to identify these argon lines before proceeding on with the identification of the iodine lines). Xenon does not have spectral lines in the vicinity of 1.3151μ , and therefore it would be a good candidate for a test gas.
3) If suggestion #1 cannot be carried out, it is suggested that the driver end of the tube be shortened from the present 15 ft (3 sections) down to one or possibly two sections. This would, in effect, reduce helium consumption by 2/3 or 1/3 respectively.
4) Use a test gas that contains iodine gas. This would dispense with the need to sublime the iodine and measure out crystalline iodine to be placed on the airfoil assembly.
5) In order to determine if sufficient energy is present to cause lasing to occur, it is suggested that a resonating cavity be established along with the means to measure output.

Bibliography

1. Barnes Engineering Co. IR Detector Test Data Sheet. Stamford, Conn. (Pamphlet included with equipment)

2. Britton, D., et al. "Shock Waves in Chemical Kinetics: Further Studies on the Rate of Dissociation of Molecular Iodine," The Journal of Chemical Physics, 25(5): (November 1956).

3. Gaydon, A.G. and I.R. Hurle. Shock Tube in High Temperature Chemical Physics. New York: Rinehold Publishing Corp., 1963.

4. Mellon, M.G. Analytical Absorption Spectroscopy; Absorptimetry and Colorimetry. New York: John Wiley & Sons, 1950.

Vita

Lt. James J. Baer was born February 19, 1955 in Superior, Wisconsin. He attended high school in 1969 in Adrian, Michigan and entered the University of Michigan, College of Engineering in fall 1973. In 1978 he graduated with a B.S. in Mechanical Engineering, and immediately went to work for the Detroit Edison Power Co. as a power plant engineer. Lt. Baer attended Officers' Training School in San Antonio, Texas in February 1980, and was commissioned a second lieutenant in the USAF in May 1980. His first assignment was at the Air Force Institute of Technology, Wright-Patterson AFB, Ohio, where he entered into a master's degree program in aeronautical engineering.

Permanent Address: 7612 Forest Ave.
Dexter, MI 48130

UNCLASSIFIED

SECURITY CLASSIFICATION OF THIS PAGE (When Data Entered)

REPORT DOCUMENTATION PAGE		READ INSTRUCTIONS BEFORE COMPLETING FORM
1. REPORT NUMBER AFIT/GAE/AA/81D-3 .	2. GOVT ACCESSION NO. AD A118 063	3. RECIPIENT'S CATALOG NUMBER
4. TITLE (and Subtitle) SPECTROGRAPHIC ANALYSIS OF IODINE EMISSION		5. TYPE OF REPORT & PERIOD COVERED Master's Thesis 6. PERFORMING ORG. REPORT NUMBER
7. AUTHOR(s) James J. Baer First Lieutenant, USAF		8. CONTRACT OR GRANT NUMBER(s)
9. PERFORMING ORGANIZATION NAME AND ADDRESS Air Force Institute of Technology (AFIT/EN) Wright-Patterson AFB, OH 45433		10. PROGRAM ELEMENT, PROJECT, TASK AREA & WORK UNIT NUMBERS
11. CONTROLLING OFFICE NAME AND ADDRESS Air Force Institute of Technology (AFIT/EN) Wright-Patterson AFB, OH 45433		12. REPORT DATE June 1982 13. NUMBER OF PAGES 55
14. MONITORING AGENCY NAME & ADDRESS(if different from Controlling Office)		15. SECURITY CLASS. (of this report) UNCLASSIFIED 15a. DECLASSIFICATION/DOWNGRADING SCHEDULE

16. DISTRIBUTION STATEMENT (of this Report)

Approved for public release; distribution unlimited.

17. DISTRIBUTION STATEMENT (of the abstract entered in Block 20, if different from Report)

AIR FORCE INSTITUTE OF TECHNOLOGY (ATC)
WRIGHT-PATTERSON AFB, OH 45433

18. SUPPLEMENTARY NOTES

Approved for public release IAW AFR 190-17

FREDRIC C. LYNCH, MAJOR, USAF
Director of Public Affairs

LYNN E. WOLAVER
Dean for Research and Professional Development
23 JUL

19. KEY WORDS (Continue on reverse side if necessary and identify by block number)

Shock Tube
Iodine-Argon Spectrum
Chemical Laser

20. ABSTRACT (Continue on reverse side if necessary and identify by block number)

The 2-inch I.D. gas dynamic shock tube at the Air Force Institute of Technology, Wright-Patterson AFB, was used to examine the infrared emission spectrum of iodine in the 1.1-1.5μ range. A reflected shock wave passing through the test gas generated the high temperature that was necessary to dissociate

DD FORM 1 JAN 73 1473 EDITION OF 1 NOV 65 IS OBSOLETE

UNCLASSIFIED

SECURITY CLASSIFICATION OF THIS PAGE (When Data Entered)

Block 20:

the iodine, and cause infrared emissions. Helium gas was used as the driver gas, and argon gas was used in the driven (test) section of the tube. The infrared emission was passed through a grating spectrometer (1200 lines/mm, 121,000 total lines) and was detected at the outlet slit with a liquid nitrogen cooled indium-antimonide IR detector. Control tests were run without iodine to verify that the spectrometer and IR detector were working properly during which time strong argon lines were observed. Subsequent tests revealed the infrared emissions characteristic of iodine in the 1.1-1.5μ range. There is sufficient evidence to suggest that the 1.3151μ electronic mode was excited; however, there may not have been a high enough energy state to extract energy in the lasing mode. The test section condition that was generated during observation of the 1.3151μ line was T_5 of approximately 5000°R.

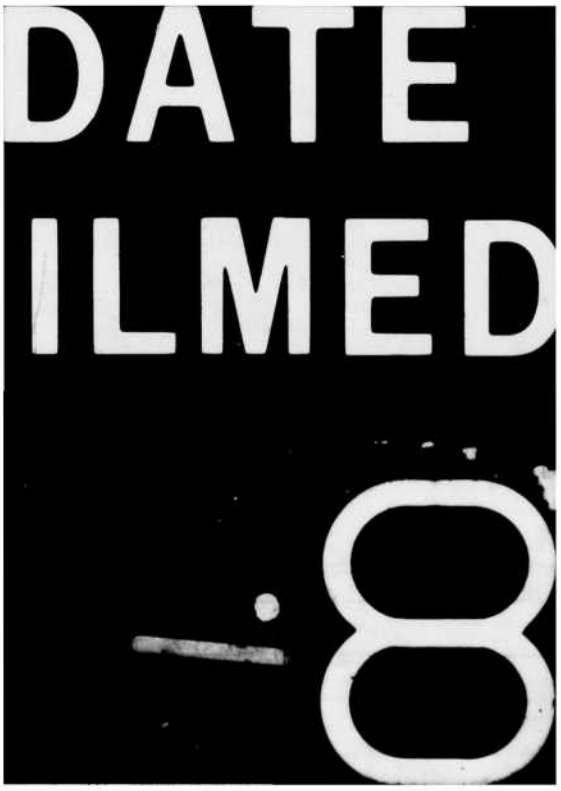
DATE
ILMED
8